Hard x-ray photoelectron spectroscopy as a probe of the intrinsic electronic properties of CdO

J. J. Mudd,[1,*] Tien-Lin Lee,[2] V. Muñoz-Sanjosé,[3] J. Zúñiga-Pérez,[4] D. Hesp,[5] J. M. Kahk,[6]
D. J. Payne,[6] R. G. Egdell,[7] and C. F. McConville[1,†]

[1]*Department of Physics, University of Warwick, Coventry, CV4 7AL, United Kingdom*
[2]*Diamond Light Source Ltd., Harwell Science and Innovation Campus, Didcot, OX11 0DE, United Kingdom*
[3]*Departamento de Fisica Aplicada y Electromagnetismo, Universitat de Valéncia, C/Dr. Moliner 50, 46100 Burjassot, Spain*
[4]*Centre de Recherche sur l' Hétéro-Epitaxie et ses Applications, Centre National de la Recherche Scientifique,*
Parc de Sophia Antipolis, Rue Bernard Grégory, 06560 Valbonne, France
[5]*Department of Physics, University of Liverpool, Liverpool, L69 3BX, United Kingdom*
[6]*Department of Materials, Imperial College London, London, SW7 2AZ, United Kingdom*
[7]*Inorganic Chemistry Laboratory, Department of Chemistry, University of Oxford, South Parks Road, Oxford OX1 3QR, United Kingdom*

Hard x-ray photoelectron spectroscopy (HAXPES) is used to investigate the intrinsic electronic properties of single crystal epitaxial CdO(100) thin films grown by metal organic vapor phase epitaxy (MOVPE). The reduced surface sensitivity of the HAXPES technique relaxes stringent surface preparation requirements, thereby allowing the measurement of as-grown samples with intrinsically higher carrier concentration ($n = 2.4 \times 10^{20}$ cm^{-3}). High-resolution HAXPES spectra of the valence band and core levels measured at photon energy of 6054 eV are presented. The effects of conduction band filling and band gap renormalization are discussed to explain the observed binding energy shifts. The measured bandwidth of the partially occupied conduction band feature indicates that a plasmon contribution may be present at higher carrier concentrations. The Cd $3d_{5/2}$ and O $1s$ core-level line shapes are found to exhibit an increased asymmetry with increased carrier concentration, interpreted as evidence for final state screening effects from the carriers in the conduction band. Alternatively the core-level line shape is interpreted as arising from strong conduction electron plasmon satellites. The nature of these two competing models to describe core-level line shapes in metallic oxides is explored.

PACS number(s): 79.60.Bm, 68.47.Gh, 71.45.Gm

I. INTRODUCTION

Oxide semiconductors such as CdO, ZnO, SnO$_2$, and In$_2$O$_3$, exhibit the normally orthogonal properties of optical transparency and high electrical conductivity, and are therefore widely used as transparent contacts [1,2]. Applications of transparent conducting oxides (TCOs) include flat screen displays, LEDs, and solar cells, the latter an application where CdO is particularly well suited [3,4]. Although this class of materials have been investigated for many years, recent improvements in epitaxial growth techniques have allowed higher quality films to be fabricated and reveal the more fundamental and intrinsic electronic properties of this class of materials [2]. One of the difficulties in probing the detailed electronic structure of TCOs using photoelectron spectroscopy is the need to prepare clean ordered surfaces under ultrahigh vacuum (UHV) conditions, after removal from a dedicated growth facility. The use of higher photon energies, and correspondingly larger probing depths, allows samples to be investigated without the strictest requirement of surface preparation necessary for lower photon energy experiments. Utilizing hard x-ray photoelectron spectroscopy (HAXPES) allows epitaxial thin films to be investigated in the "as-grown" condition [5]. This is especially useful in the case of materials such as CdO which are often prepared *in-situ* by high temperature annealing (>500 °C), a process

which typically results in a lowering of the samples carrier concentration ($n < 3 \times 10^{19}$ cm^{-3}) [6,7].

The photoelectron inelastic mean free path (IMFP) is significantly enhanced using hard x rays. For example, valence electrons with a binding energy of 2 eV escape from a depth of ∼20 nm using a photon energy of 6054 eV compared to ∼6 nm for an Al K_α laboratory source ($h\nu = 1486$ eV), as calculated using a TPP-2M formula [8]. Higher photon energies result in decreased surface sensitivity, although the experiment becomes significantly more challenging as a result of reduced photoionization cross sections. For example, the Cd $3d$ cross section decreases by a factor of ∼100 on moving from 1486 to 6054 eV [9]. This can, however, be overcome using a third generation synchrotron source to provide extremely high photon fluxes, combined with recent advances in electron analyzers which enables more efficient photoelectron detection. The aim of this paper is to show that detailed intrinsic electronic properties of CdO can be obtained without requiring surface preparation by utilizing HAXPES.

II. EXPERIMENTAL AND THEORETICAL DETAILS

Epitaxial CdO(100) single crystal thin films were grown on r-plane sapphire substrates using metal organic vapor-phase epitaxy (MOVPE), further details of which can be found elsewhere [10]. A comparison was made between samples taken from the same wafer, one annealed in UHV at 600 °C for 1 h to lower the carrier concentration, likely resulting from the removal of hydrogen [11], or Cd intersticials. Hall effect measurements of these samples taken following the HAXPES experiment revealed a carrier concentration

---
*j.j.mudd@warwick.ac.uk
†c.f.mcconville@warwick.ac.uk

of $n = 2.4 \times 10^{20}$ cm^{-3} and mobility of $\mu = 43$ cm^2 V^{-1} s^{-1} for the as-grown sample, and $n = 1.8 \times 10^{19}$ cm^{-3}, $\mu = 110$ cm^2 V^{-1} s^{-1} for the UHV annealed sample. The HAXPES experiments were conducted at beamline I09, Diamond Light Source, UK. This beamline offers photon energies from 230 eV to 18 keV, while the endstation is equipped with a VG Scienta EW4000 electron analyzer with ±30° angular acceptance. For hard x rays a channel cut Si(004) crystal was used following the Si double crystal monochromator to further improve the beamline energy resolution, resulting in a photon energy of 6054 eV and overall energy resolution <250 meV. The soft x ray were monochromated using a plane grating monochromator giving a energy resolution of ~300 meV. Switching between photon energies is achieved without moving the sample. The photoemission measurements were performed at room temperature, and the binding energy scale was calibrated to the Fermi edge cutoff.

To model conduction band filling a two band $\mathbf{k} \cdot \mathbf{p}$ carrier statistics model was used [12], with material parameters consisting of a direct band gap of 2.20 eV, and a bulk conduction band effective mass of $0.24m_0$ [13]. This results in a Fermi level of 0.52 eV (0.09 eV) above the conduction band minimum (CBM) for the as-grown (annealed) CdO samples, respectively. This is illustrated schematically in Fig. 2(a).

III. RESULTS AND DISCUSSION

A. Surface sensitivity

Figure 1 shows a comparison between the O 1s and Cd 3d core levels taken using hard and soft x-ray photoemission spectroscopy (HAXPES and SXPES). Due to the lower photon energy the SXPES (600 eV) data are much more surface

FIG. 1. (Color online) Comparison of HAXPES and SXPES taken using photon energies of 6054 and 600 eV, respectively. (a) O 1s, (b) Cd 3d for the annealed sample ($n = 1.8 \times 10^{19}$ cm^{-3}) and (c) O 1s, (d) Cd 3d for the as-grown sample ($n = 2.4 \times 10^{20}$ cm^{-3}).

sensitive than the HAXPES (6054 eV) data. This is most clearly illustrated by the contamination peak in the O 1s region, Figs. 1(a) and 1(c) at ~531.5 eV, which is strongly enhanced on both the as-grown and annealed samples with the lower photon energy, and is assigned principally to CdCO$_3$ [14], but also contains atmospheric contamination components. In the O 1s spectra of the as-grown sample, this contamination peak dominates the spectrum and is not clearly resolved from the CdO peak, making line shape analysis very difficult and unreliable. This situation is greatly improved by employing high photon energies where the sensitivity to the surface and therefore the contamination components are greatly reduced, and by fitting can easily be separated from the main peak. The situation is very similar in the Cd 3d region, where only a peak shift due to the band bending, and a broadening due to reduced experimental resolution are observed on the annealed sample and no significant contamination component is visible. However, the as-grown sample displays a large contamination component at ~405.1 eV, on the Cd 3$d_{5/2}$ assigned to CdCO$_3$ or Cd(OH)$_2$ [15]. This component dominates the spectra, in this case, making the core-level shape appear almost mirrored. This component is again greatly reduced by the higher photon energy, allowing the core-level line shape to be analyzed, while still incorporating the reduced contamination component when preforming peak fitting.

The peak shifts observed in Fig. 1(b) and in the CdO component of the O 1s region are assigned to the band bending present at CdO surfaces. The lower photon energy enhances surface sensitivity, and as CdO exhibits downward band bending a peak shift to higher binding energy should be expected, an effect recently exploited in an investigation of SnO$_2$ [16]. The peak shifts observed here are ~0.4 eV, consistent with the large downward band bending previously observed on CdO [6,7].

This illustrates the difficulties in accessing electronic properties of as-grown CdO samples with SXPES and how this situation is significantly improved by the application of HAXPES.

B. Valence band

The valence band region for the as-grown and annealed samples is shown in Fig. 2(b). A binding energy shift due to conduction band (CB) filling is clearly visible, and by linear extrapolation of the leading edge, the valence band maximum (VBM) to Fermi level separation (ξ) was found to be 1.29 ± 0.07 and 0.99 ± 0.07 eV for the as-grown (higher carrier concentration) and annealed (lower carrier concentration) samples, respectively. This gives a VBM shift of 0.30 ± 0.10 eV, which is less than the predicted shift of 0.43 eV from carrier statistics. This discrepancy can be understood if band gap renormalization (BGR) is taken into account [17–19]. A band gap shrinkage of 0.07 and 0.20 eV is predicted for the low and high carrier concentrations, respectively [20]. This would then imply a VBM shift of 0.30 eV, which is in excellent agreement with the experimental result, illustrating the bulk-like sensitivity of the technique. Just below the Fermi level a small feature is clearly visible, shown magnified (×50) in Fig. 2(b), this is assigned to photoelectrons from CB states. The intensity of this feature is significantly enhanced for the as-grown sample, as would be expected in the case of increased bulk CB filling. The
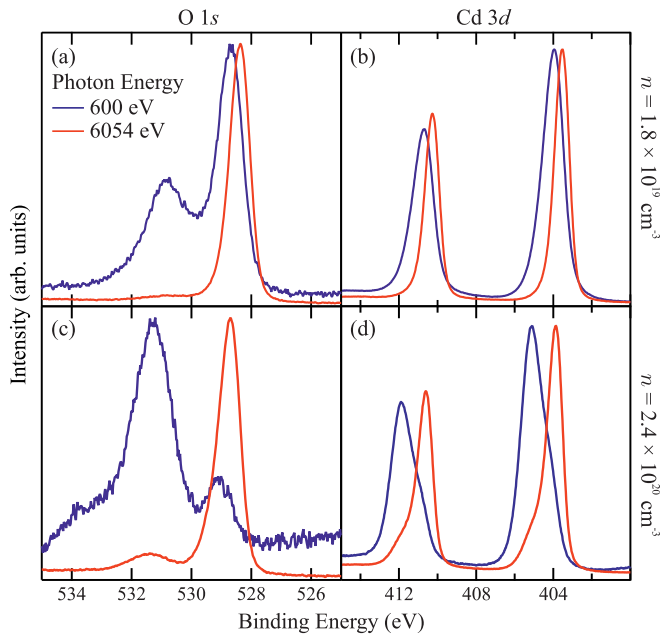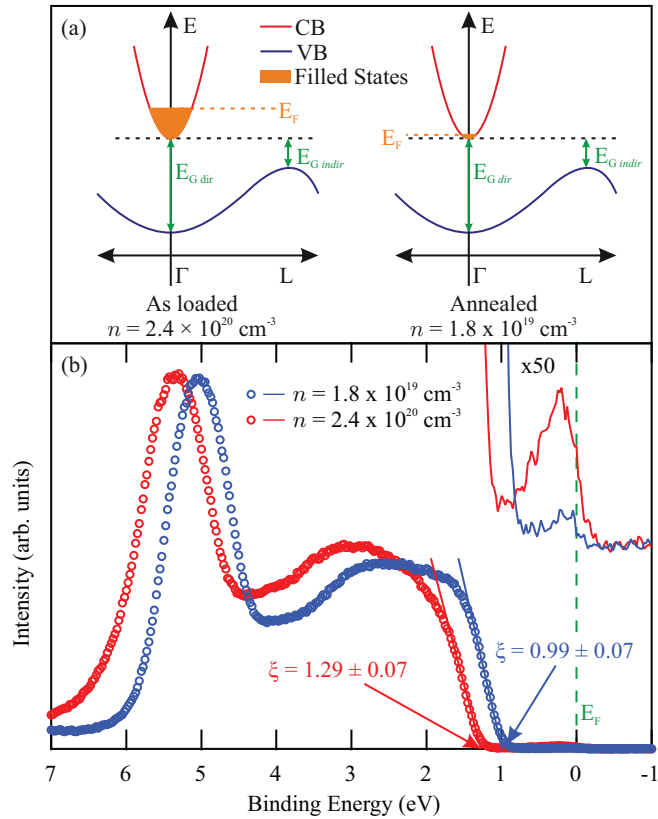
FIG. 2. (Color online) (a) A band schematic for a high and low carrier concentration, illustrating the band filling and indirect band gap. (b) HAXPES valence band spectra for the as-grown ($n = 2.4 \times 10^{20}$ cm^{-3}, red) and annealed ($n = 1.8 \times 10^{19}$ cm^{-3}, blue) samples. Extrapolations of the VB leading edge are shown. Magnified ($\times 50$) and offset spectra (solid line) are also shown allowing the CB intensity just below the Fermi level (E_F) to be visible.

FIG. 3. (Color online) Cd $3d$ spectra shown for the as-grown ($n = 2.4 \times 10^{20}$ cm^{-3}, red) and annealed ($n = 1.8 \times 10^{19}$ cm^{-3}, blue) samples. A symmetric Voigt peak shape is also shown as a reference to allow the asymmetry to be observed.

bandwidth of this feature is 0.7 ± 0.1 eV for the as-grown sample and 0.4 ± 0.2 eV for the annealed sample. These values are both significantly in excess of the predicted CB filling using measured Hall carrier concentration and carrier statistics, indicating that extra electrons at deeper binding energies are present. There are two possible explanations. First, the CB feature could incorporate a plasmon satellite, as has been observed previously on Na$_x$WO$_3$ and simple metals [21,22]. Alternatively, clean CdO surfaces are known to exhibit downward band bending and associated electron accumulation, giving rise to quantized surface states at higher binding energies than present in the bulk [6,7]. These two possibilities are discussed later in the context of the core-level line shapes. Both the CB state and valence feature at ∼5.5 eV are strongly enhanced relative to the top of the VB, compared to previous lower photon energy measurements [14,15]. This is due to the pronounced Cd $5s$ character of both states which exhibit a slower decrease in photoionization cross section with increasing photon energy than either the O $2p$ or Cd $4d$ states which compose the rest of the valence band [15,23].

C. Core levels

The Cd $3d$ and O $1s$ core levels have been investigated to assess the effects of final state effects on the core-level line
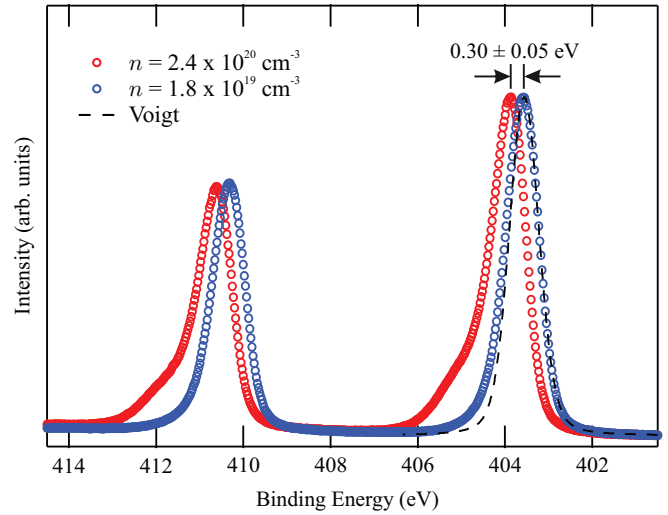
shape. In principle, the Cd $4d$ peak should also exhibit a similar phenomenon. However, the Cd $4d$ levels in CdO are extremely shallow (∼10 eV) and hybridize strongly with the O $2p$ levels complicating detailed peak fitting [15,24]. Therefore, we have directed our focus on the Cd $3d$ and O $1s$ core levels.

Cd $3d$ spectra for both carrier concentrations are shown in Fig. 3, a 0.30 ± 0.05 eV binding energy (BE) shift arising from upward movement of the Fermi level within the CB as the carrier concentration increases. This is in excellent agreement with the observed shift in the VBM shown in Fig. 2(b). This shift is again smaller than predicted by carrier statistics, indicating the importance of considering BGR in this material. The measured peak shape also exhibits significant asymmetry, compared to a symmetrical Voigt peak fitted to the low BE side of the Cd $3d_{5/2}$ peak. It should be noted that for higher carrier concentration a more significant shoulder is observed on the high BE side of the peak [15]. This asymmetry is caused by final state screening effects, which can be enhanced due to the downward band bending and associated electron accumulation present at the surface, previously observed for SnO$_2$, In$_2$O$_3$, and InN [25–28].

Two different models have been proposed to account for core-level line shapes observed in photoemission spectra from so-called narrow-band metallic oxides [29]. The first model, introduced to account for core-level line shapes in sodium tungsten bronze (Na$_x$WO$_3$) [21,30], recognizes that when the Coulomb interaction between a core hole and an orbital contributing to the conduction band exceeds the occupied conduction bandwidth, the potential associated with the core hole will create a localized state on the ionized atom. Two different finals states are then accessible, depending on whether the localized state becomes occupied to give a screened final state or remains empty to give an unscreened final state. Within this model the probability of final state screening should increase with increasing carrier density, and peaks associated with unscreened final states will be broadened by lifetime effects to give a characteristically Lorentzian line
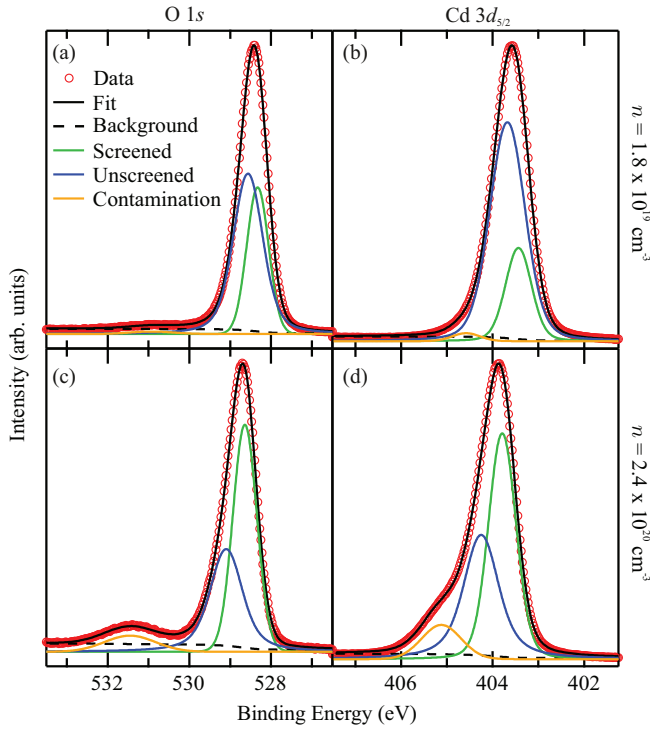
FIG. 4. (Color online) HAXPES spectra and fits for (a) O $1s$, (b) Cd $3d_{5/2}$ for the annealed sample ($n = 1.8 \times 10^{19}$ cm^{-3}). (c) O $1s$, (d) Cd $3d_{5/2}$ for the as-grown sample ($n = 2.4 \times 10^{20}$ cm^{-3}). Fits were preformed using three Voigt line shapes and a Shirley background, the assignment of the peaks is discussed in the text.

shape. The alternative model treats the low binding energy component as the "main" peak, while the higher binding energy peak is an unusually strong plasmon satellite broadened by the conduction electron scattering rate. The theory of plasmon satellites in low electron density metals suggests that the intensity of the high binding satellites should increase with decreasing electron density n according to an $n^{-1/3}$ power law [21]. For a number of closely related systems such as Sb-doped SnO$_2$ [25], PbO$_{2-x}$ [31], and Sn-doped In$_2$O$_3$ [27] it has been shown that satellite energies are indeed close to plasmon energies measured by infrared reflectance spectroscopy or electron energy loss spectroscopy. It remains a challenge to theory to reconcile these two apparently distinct models, which nonetheless produce rather similar qualitative conclusions, i.e. increased intensity of the low binding energy

component with increasing carrier density and a lifetime broadened line shape for the high binding energy component.

Figures 4(a) and 4(b) show curve fits to the O $1s$ and Cd $3d_{5/2}$ core lines for the annealed (lower carrier concentration) sample, while the corresponding fits for the sample with higher carrier concentration are shown in Figs. 4(c) and 4(d). The fitting for all peaks was preformed using three Voigt line shapes with a Shirley background. The binding energies and relative intensities derived from the curve fits are summarized in Table I. The third component at higher binding energy is associated with surface contamination [possibly CdCO$_3$ or Cd(OH)$_2$]. As expected, this component is much weaker for the low carrier density sample that has been annealed. Several aspects of the curve fits deserve comment. First, the spectral weight associated with the low binding energy main or screened peak is higher for the sample with higher carrier density in both the Cd $3d_{5/2}$ and O $1s$ regions, as expected from the discussion above. Second, the energy separation between the screened and unscreened peaks (main and plasmon satellite, in the plasmon model) is consistent for curve fits of the two different core lines and is larger for the higher carrier density (as-grown) sample. Third, there is a well defined shift to higher binding energy for the sample with higher carrier density, as expected from increased occupation of the conduction band discussed previously. Finally, the relative intensity of the high binding energy component is weaker in the O $1s$ region than in the Cd $3d_{5/2}$ region for both samples. This observation is qualitatively consistent with the plasmon model because conduction band states in CdO are of predominantly Cd $5s$ character with a weaker O $2p$ contribution arising from O $2p$–Cd $5s$ hybridization, so that a cadmium core hole is more likely to excite plasmons than an oxygen core hole. It is more difficult to understand the intensity differences utilizing the final state screening model. We note that previous interpretations of core line shapes in CdO were based on the proposed existence of CdO$_2$ as a surface phase [14]. The present experiments lead to a revision of this assignment as the surface contribution in HAXPES is very much lower than in conventional photoemission but nonetheless the satellites remain strong.

If the two peaks are interpreted as a main peak and a plasmon satellite, the splitting of the two components can be used to obtain a carrier density n using

$$E_p = \hbar \left(\frac{ne^2}{m^* \varepsilon_0 \varepsilon(\infty)} \right)^{1/2}, \tag{1}$$

TABLE I. Peak fitting results for Cd $3d_{5/2}$ and O $1s$ core levels, split by carrier concentration and component. The contamination peaks have been excluded for the relative area calculation. E_P is the plasmon energy, the separation between the screened and unscreened components.

Peak	n (cm^{-3})	Component	BE (± 0.05 eV)	FWHM (± 0.05 eV)	Rel. Area (%)	E_p (meV)
Cd $3d_{5/2}$	1.8×10^{19}	Screened	403.43	0.67	24	
		Unscreened	403.68	0.90	76	250
Cd $3d_{5/2}$	2.4×10^{20}	Screened	403.79	0.71	55	
		Unscreened	404.25	0.90	45	460
O $1s$	1.8×10^{19}	Screened	528.33	0.66	45	
		Unscreened	528.57	0.88	55	240
O $1s$	2.4×10^{20}	Screened	528.64	0.69	57	
		Unscreened	529.10	0.93	43	460

here E_p is the plasmon energy, $\varepsilon(\infty)$ is the high frequency dielectric constant, and m^* is the effective mass at the Fermi level. Using a band edge effective mass of $m^* = 0.24m_0$ and $\varepsilon(\infty) = 5.4$ [13,32], a plasmon energy of $E_p = 245$ meV for the annealed sample gives a carrier density of $n = 5.9 \times 10^{19}$ cm^{-3}, whereas $E_p = 460$ meV for the as-grown sample gives $n = 2.5 \times 10^{20}$ cm^{-3}. The agreement with Hall measurement is excellent for the high carrier concentration sample, illustrating HAXPES bulk sensitivity, and suggests there is no significant contribution of extra carrier density from an electron accumulation layer. This in turn suggests the large bandwidth of the observed CB feature is more likely due to a plasmon satellite. Additionally a bandwidth of 0.7 ± 0.1 eV would be consistent with a 460 meV plasmon separation observed on the core levels. For the annealed sample the carrier density obtained from the plasmon separation is notably higher than that obtained from Hall measurement. This indicates an electron accumulation layer plays a significant role in the final state screening, as would be expected when it contributes a significant fraction of the electron density within the first 20 nm. It is therefore likely that there is both a plasmon and surface electron accumulation contribution to the observed bandwidth.

IV. CONCLUSIONS

HAXPES has been used to study the intrinsic electronic properties of CdO(100) single crystal thin films. The use of higher energy photons allowed the CdO thin films to be studied in as-grown conditions with the associated higher carrier concentrations. The effects of CB filling on the Fermi level position were clearly observed, and band gap renormalization was found to be significant when analyzing the VBM and core-level shifts. The effects of CB plasmons, or final state screening on the core-level line shapes, was observed, revealing a dependence on the carrier concentration. The plasmon energy extracted using peak fits was converted to carrier density and showed excellent agreement with the Hall measurement for the as-grown sample. This supports the result that the observed bandwidth of the CB state on the as-grown sample may be due to a plasmon satellite. For the annealed sample the plasmon energy indicated a higher carrier concentration than obtained from Hall measurement, suggesting electron accumulation is playing a significant role in the final state screening effects. Further theoretical work should be directed at modeling the core-level line shape in such systems to allow the competing effects to be truly disambiguated.

The observation of these intrinsic electronic properties despite no surface preparation show HAXPES is a powerful technique for the investigation of oxide semiconducting materials, especially where *in situ* preparation and surface treatment can otherwise significantly alter the intrinsic material properties. This is common in TCOs where unintentional doping and surface conductivity appears to be a defining characteristic of the materials [2].

[1] D. S. Ginley and C. Bright, MRS Bull. **25**, 15 (2000).

[2] P. D. C. King and T. D. Veal, J. Phys.: Condens. Matter **23**, 334214 (2011).

[3] K. M. Yu, M. A. Mayer, D. T. Speaks, H. He, R. Zhao, L. Hsu, S. S. Mao, E. E. Haller, and W. Walukiewicz, J. Appl. Phys. **111**, 123505 (2012).

[4] T. J. Coutts, D. L. Young, X. Li, W. P. Mulligan, and X. Wu, J. Vac. Sci. Technol. A **18**, 2646 (2000).

[5] G. Panaccione and K. Kobayashi, Surf. Sci. **606**, 125 (2012).

[6] L. F. J. Piper, L. Colakerol, P. D. C. King, A. Schleife, J. Zúñiga-Pérez, P.-A. Glans, T. Learmonth, A. Federov, T. D. Veal, F. Fuchs, V. Muñoz-Sanjosé, F. Bechstedt, C. F. McConville, and K. E. Smith, Phys. Rev. B **78**, 165127 (2008).

[7] P. D. C. King, T. D. Veal, C. F. McConville, J. Zúñiga-Pérez, V. Muñoz-Sanjosé, M. Hopkinson, E. D. L. Rienks, M. F. Jensen, and P. Hofmann, Phys. Rev. Lett. **104**, 256803 (2010).

[8] S. Tanuma, C. Powell, and D. R. Penn, Surf. Interface Anal. **21**, 165 (1994).

[9] J. Scofield, Lawrence Livermore Laboratory, Report No. UCRL-51326 (1973).

[10] J. Zúñiga-Pérez, C. Munuera, C. Ocal, and V. Muñoz-Sanjosé, J. Cryst. Growth **271**, 223 (2004).

[11] P. D. C. King, T. D. Veal, P. H. Jefferson, J. Zúñiga-Pérez, V. Muñoz-Sanjosé, and C. F. McConville, Phys. Rev. B **79**, 035203 (2009).

[12] E. O. Kane, J. Phys. Chem. Solids **1**, 249 (1957).

[13] S. K. Vasheghani Farahani, T. D. Veal, P. D. C. King, J. Zúñiga-Pérez, V. Muñoz-Sanjosé, and C. F. McConville, J. Appl. Phys. **109**, 073712 (2011).

[14] L. F. J. Piper, P. H. Jefferson, T. D. Veal, C. F. McConville, J. Zúñiga-Pérez, and V. Muñoz-Sanjosé, Superlattice. Microst. **42**, 197 (2007).

[15] P. D. C. King, T. D. Veal, A. Schleife, J. Zúñiga-Pérez, B. Martel, P. H. Jefferson, F. Fuchs, V. Muñoz-Sanjosé, F. Bechstedt, and C. F. McConville, Phys. Rev. B **79**, 205205 (2009).

[16] T. Nagata, O. Bierwagen, M. E. White, M. Y. Tsai, Y. Yamashita, H. Yoshikawa, N. Ohashi, K. Kobayashi, T. Chikyow, and J. S. Speck, Appl. Phys. Lett. **98**, 232107 (2011).

[17] S. K. Vasheghani Farahani, V. Muñoz-Sanjosé, J. Zúñiga-Pérez, C. F. McConville, and T. D. Veal, Appl. Phys. Lett. **102**, 022102 (2013).

[18] K. F. Berggren and B. E. Sernelius, Phys. Rev. B **24**, 1971 (1981).

[19] D. T. Speaks, M. A. Mayer, K. M. Yu, S. S. Mao, E. E. Haller, and W. Walukiewicz, J. Appl. Phys. **107**, 113706 (2010).

[20] S. K. Vasheghani Farahani (private communication).

[21] J. N. Chazalviel, M. Campagna, G. K. Wertheim, and H. R. Shanks, Phys. Rev. B **16**, 697 (1977).

[22] P. Steiner, H. Hochst, and S. Hüfner, *Photoemission in Solids II* (Springer, Berlin, 1979), pp. 349–372.

[23] M. Burbano, D. O. Scanlon, and G. W. Watson, J. Am. Chem. Soc. **133**, 15065 (2011).

[24] Y. Dou, R. G. Egdell, D. S. L. Law, N. M. Harrison, and B. G. Searle, J. Phys.: Condens. Matter **10**, 8447 (1998).

[25] R. G. Egdell, J. Rebane, T. J. Walker, and D. S. L. Law, Phys. Rev. B **59**, 1792 (1999).

[26] C. Körber, V. Krishnakumar, A. Klein, G. Panaccione, P. Torelli, A. Walsh, J. L. F. Da Silva, S.-H. Wei, R. G. Egdell, and D. J. Payne, Phys. Rev. B **81**, 165207 (2010).

[27] A. Bourlange, D. J. Payne, R. G. Palgrave, H. Zhang, J. S. Foord, R. G. Egdell, R. M. J. Jacobs, T. D. Veal, P. D. C. King, and C. F. McConville, J. Appl. Phys. **106**, 013703 (2009).

[28] P. D. C. King, T. D. Veal, H. Lu, S. A. Hatfield, W. J. Schaff, and C. F. McConville, Surf. Sci. **602**, 871 (2008).

[29] N. Beatham, P. Cox, R. Egdell, and A. Orchard, Chem. Phys. Lett. **69**, 479 (1980).

[30] M. Campagna, G. K. Wertheim, H. R. Shanks, F. Zumsteg, and E. Banks, Phys. Rev. Lett. **34**, 738 (1975).

[31] D. J. Payne, R. G. Egdell, W. Hao, J. S. Foord, A. Walsh, and G. W. Watson, Chem. Phys. Lett. **411**, 181 (2005).

[32] W. W. H. Finkenrath and N. Uhle, Solid State Commun. **7**, 11–14 (1969).